

A cycle-by-cycle fatigue damage analysis of biaxial composite structures utilizing acoustic emission

Zarouchas, D. S.; Pascoe, J.A.; Alderliesten, R. C.

Publication date

2020

Document Version

Final published version

Published in

ECCM 2018 - 18th European Conference on Composite Materials

Citation (APA)

Zarouchas, D. S., Pascoe, J. A., & Alderliesten, R. C. (2020). A cycle-by-cycle fatigue damage analysis of biaxial composite structures utilizing acoustic emission. In *ECCM 2018 - 18th European Conference on Composite Materials* (ECCM 2018 - 18th European Conference on Composite Materials). Applied Mechanics Laboratory.

Important note

To cite this publication, please use the final published version (if applicable).
Please check the document version above.

Copyright

Other than for strictly personal use, it is not permitted to download, forward or distribute the text or part of it, without the consent of the author(s) and/or copyright holder(s), unless the work is under an open content license such as Creative Commons.

Takedown policy

Please contact us and provide details if you believe this document breaches copyrights.
We will remove access to the work immediately and investigate your claim.

A CYCLE-BY-CYCLE FATIGUE DAMAGE ANALYSIS OF BIAXIAL COMPOSITE STRUCTURES UTILIZING ACOUSTIC EMISSION

D.S. Zarouchas¹, J.A. Pascoe² and R.C. Alderliesten³

¹Structural Integrity & Composites Group, Delft University of Technology,
Kluyverweg 1 2629HS, the Netherlands

Email: d.zarouchas@tudelft.nl , Web Page: <https://www.tudelft.nl/staff/d.zarouchas/>

²Department of Aeronautics, Imperial College London, South Kensington Campus,
London, SW7 2AZ, United Kingdom

Email: j.pascoe@imperial.ac.uk , Web Page: <http://www.imperial.ac.uk/people/j.pascoe>

³Structural Integrity & Composites Group, Delft University of Technology,
Kluyverweg 1 2629HS, the Netherlands

Email: r.c.alderliesten@tudelft.nl , Web Page: <https://www.tudelft.nl/staff/r.c.alderliesten/>

Keywords: fatigue damage accumulation, acoustic emission, cycle-by-cycle analysis

Abstract

In the present work, a fatigue damage analysis of biaxial Carbon Fibre Reinforced Polymer (CFRP) specimens loaded at two different stress levels and a fatigue ratio, $R=0.1$, was performed. A cycle-by-cycle approach was used, utilizing results from Acoustic Emission (AE) measurements. The aim was to investigate the influence of the applied maximum stress level on the fatigue damage accumulation process and to examine the hypothesis that damage growth occurs in a portion of a load cycle. It was found that the damage process, for the specimens loaded in lower applied stress, was gradually increased where different damage mechanisms evolved slowly towards the end of life. On the other hand, for the specimens loaded in higher applied stress, the damage process accumulated evenly and several failure mechanisms occurred in parallel at a very early stage of the fatigue life. Finally, for both loading cases, a load threshold was found, below which, there was no damage growth, supporting the hypothesis of this work.

1. Introduction

Fatigue damage in composite structures is a multi-state degradation process where several damage mechanisms, -i.e. matrix cracking, delamination, fibre breakage and pull-out- occur, interact and lead to final failure. A significant number of studies has been performed over the last decades where the research community investigated the fatigue damage process. The main conclusion was that the type of the individual damage mechanisms and sequence of their occurrence and interaction depend on the material type, lay-up, loading, manufacturing process and environmental conditions. This hypothesis that was made by Reifsneider et al. in the early '80s and thoroughly discussed by Harris at the beginning of '00s [1,2].

A common three-stage damage process has been identified for unidirectional, cross-ply and angle-ply composites [3,4];

- stage I - damage initiation by formation of matrix cracking with numerous micro-cracks developed within the ply-level until saturation,

- stage II – damage progression in the matrix-fibre phase resulting in fibre debonding and in parallel formation of delaminations
- stage III – fibre breakage and pull-out, which eventually leads to the final failure.

Although a common trend was found, the precise process of fatigue damage accumulation and consequently the underlying physical phenomena are still unknown. Let's consider that the initiation and propagation of different damage mechanisms form the overall damage growth process within the course of a fatigue cycle. As these damage mechanisms are activated individually or synergistically affecting each other, and one mechanism can be dominant during a period of the fatigue life and a different mechanism on a different period, it is logical to hypothesize that the damage growth changes every cycle. Similar hypothesis was made by the authors where they examined the fatigue crack growth on adhesively bonded structures, rationalizing that as long as the imposed fatigue load changes during the fatigue life, the crack growth rate should not be constant [5]. They used AE technique to pin-point at which part of the fatigue cycle the crack growth took place. They found evidence that the crack growth didn't occur only at the maximum load, but it didn't also occur near the minimum load. Finally they observed that the crack growth occurred in a portion of the fatigue cycle above a certain threshold value. They argued that this threshold depends on the load history and the testing frequency.

A similar analysis was adopted in this study where the aim was to investigate the influence of the applied maximum stress level, for a given R ratio, on the fatigue damage accumulation process and to examine the hypothesis that damage growth occurs in a portion of a load cycle. The paper is organized as follows: Section 2 presents the material used for this study, the fatigue tests and AE equipment. Section 3 presents the results and discusses the relation between the damage accumulation with the AE activity and the damage development over a fatigue loading range. Finally, conclusions are drawn in section 4.

2. Material and Experimental method

The material used for manufacturing of the specimens is a Hexcel AS4/8552 unidirectional prepreg ply. The AS4 fibres are continuous carbon fibres while the HexPly 8552 resin is an amine cured epoxy resin. A 600x600mm laminate with an average thickness of 2.285mm and a $[\pm 45]_{4S}$ lay-up was manufactured from the AS4/8552 prepreg. A hand lay-up was conducted and a debulking procedure was performed after every 3 plies. After lay-up, the laminate was cured in an autoclave following a cycle recommended by the manufacturer. After curing, the laminate was cut using a Proth Industrial liquid-cooled saw to obtain rectangular specimens of 250mmx25mm dimensions.

An AMSY-6 Vallen, 8-channel Acoustic Emission (AE) system with 4 parametric input channels was used in order to perform the AE measurements. Two wide-band piezoelectric sensors, AE1045S, with external 34 dB pre-amplifier and band-pass filters of 20-1200 kHz, were clamped on the specimens using mechanical holders. Grease was applied on the surface of the sensors, in order to increase the conductivity between the AE sensor and the specimen. The distance of the two sensors was 100mm and the wave speed was measured as 4.6E03 m/s by performing several pencil breaks. Attenuation of the wave propagation was measured and it was found to be insignificant for the 100mm distance. Before each test, pencil break tests were conducted close to the sensors so as to ensure a sufficient contact between the sensors and the coupons. One parametric input channel was used to record the load and correlate it to the AE data.

Initially, the tensile strength of the $[\pm 45]_{4S}$ laminate was measured by testing five coupons under displacement control with a head-displacement rate of 1.5mm/min. The fatigue tests were performed using a load-control mode with frequency 5 Hz and all specimens were tested until failure. Two load levels were selected, corresponding to the 55% and 75% of the tensile strength of the laminate. Both quasi-static and fatigue tests were executed in a MTS 60 kN test frame.

3. Results and discussion

In total 14 specimens were tested and 3 failed in or very close to the clamps. The results of those 3 specimens were not analyzed. AE was continuously recording and the acquisition threshold was set to 50 dB. Each AE data set contained the waveform of every AE hit, its duration and rise time (μsec), its peak amplitude (dB) and energy (eu) and finally the counts (number of threshold crossings). Finally, a flag was used to assign each AE hit to the loading phase and load value. The acoustic emission activity was similar for the specimens tested at the same stress level and results from one specimen per stress level will be presented hereafter. AE hits that were localized by the two AE sensors were considered for analysis. A typical AE fatigue data set ranges from 10^4 - 10^7 hits, but it should be noted that the number of hits depends on the settings used in the AE data acquisition system.

The cumulative number of AE hits has been the common way of studying the fatigue damage process as it gives an indication of how much damage is accumulated during the fatigue life of the composite structure. However, this analysis only provides information on the macroscale level, excluding any information about the failure mechanisms involved. It is well known that when damage occurs, for example due to matrix cracking, an elastic waveform is generated with signal features, i.e. amplitude, duration, frequency etc. different from the waveforms generated from other failure mechanisms such as delamination or matrix-to-fibre debonding. Thus, it is worth to examine how these signal characteristics evolve during the fatigue life and try to relate it in a qualitative manner with the failure mechanisms. This will be further discussed in the following section.

3.1 Acoustic emission activity

As it was discussed in the introduction, fatigue damage accumulates in the composite structure in the form of several failure mechanisms which are activated individually or synergistically. Each failure mechanism has a characteristic AE waveform, seen as signature, with different signal features. Several researchers investigated them and reported that they have the following generic characteristics, see for example [6,7]:

- Matrix cracking waveform has relatively long duration and rise time, low amplitude and energy
- Delamination waveform has long duration and rise time and relative high energy
- Matrix-fibre debonding waveform has relatively short duration and low energy
- Fibre breakage waveform has very short duration and rise time, high amplitude and energy.

The acoustic emission activity over the fatigue time is presented in figures 1-4, for two specimens loaded at the two σ_{max} . Figure 1 and 2 present the distribution of peak amplitudes, duration, energy and rise time of the signals which were recorded during the loading and unloading phases of the fatigue cycles respectively for a specimen loaded at 55%. The results were averaged per a time window of 50 sec.

The averaged amplitude is rather low and it fluctuates during the first half of the specimen's fatigue life. The two peaks close to 30% and 50% of the fatigue life show a rapid accumulation of damage and in combination with the results for the duration, energy and rise time, the damage can be attributed to matrix cracking saturation that occurs at the 30% of the fatigue life and the formation of delamination. During the second half of the fatigue life, the amplitude is leveled to a low value while the duration, rise energy and rise time increase, indicating the development of more delamination and the propagation of existing delaminations towards the final failure of the specimen.

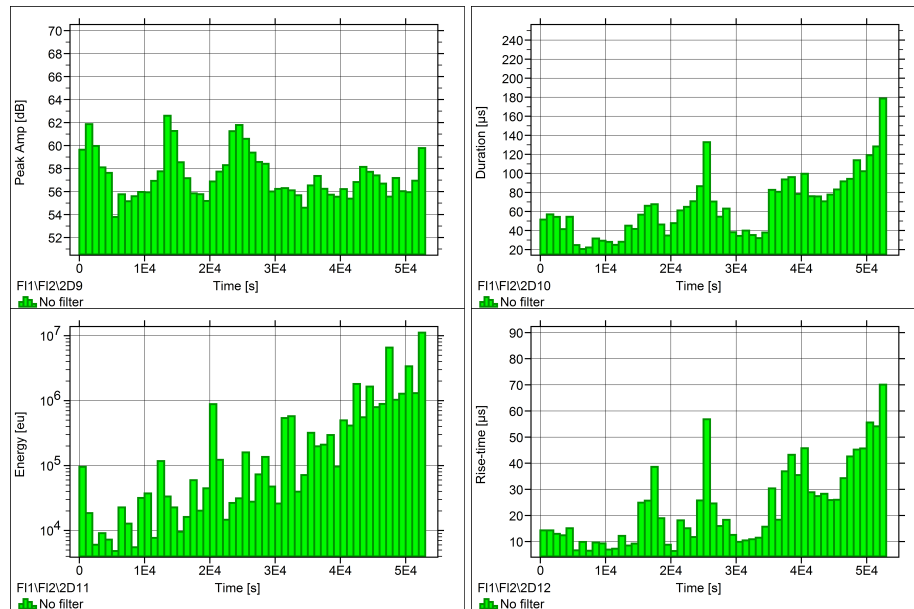


Figure 1. Acoustic emission activity for the loading phase: Peak Amp (upper left), Duration (upper right), Energy (lower left), Rise-time (lower right)

For the unloading phase, the averaged amplitude is again low and fairly constant during the fatigue life. The energy distribution behaves similarly. On the other hand, the duration and rise time are constantly increasing during the fatigue life. Although, it is expected that new damage formation occurs during the loading phase, there is a possibility that damage is created during the unloading phase as well.

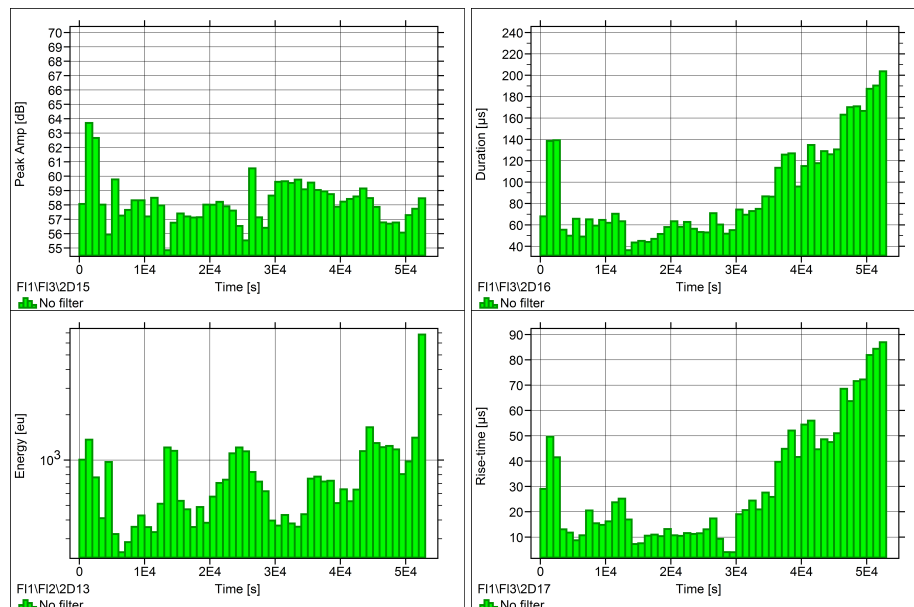


Figure 2. Acoustic emission activity for the unloading phase: Peak Amp (upper left), Duration (upper right), Energy (lower left), Rise-time (lower right)

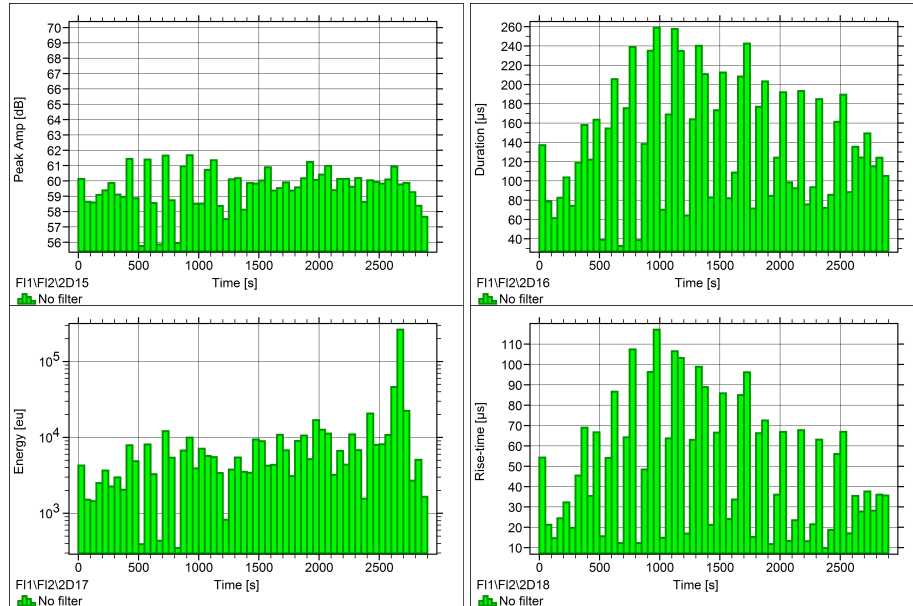
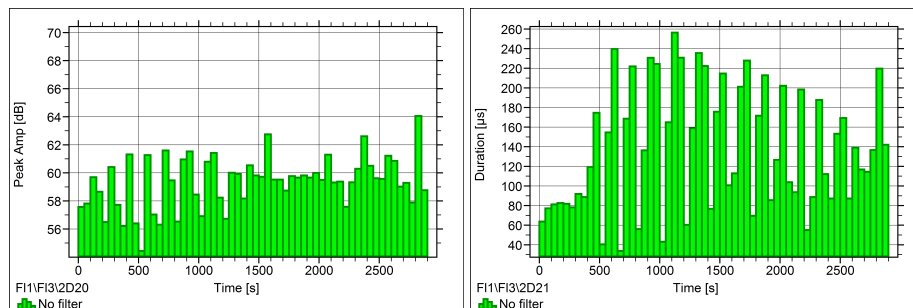


Figure 3. Acoustic emission activity for the loading phase: Peak Amp (upper left), Duration (upper right), Energy (lower left), Rise-time (lower right)

Similarly, Figures 3 and 4 present the distribution of peak amplitudes, duration, energy and rise time of the signals which were recorded during the loading and the unloading phase of the fatigue cycles for the specimen, loaded at 75%.

The averaged amplitude is again low and there are cycles between 20% and 30% of the fatigue life where the AE activity is almost zero, meaning that during those cycles, damage growth is insignificant. Similar behavior was not observed in the previous specimen. Furthermore, the distribution rate of duration and rise time increase very early to values which could be associated to delamination and friction phenomena. This means that for specimens loaded in high σ_{\max} delamination may occur much earlier in their fatigue life. It is notable that in between the long duration and rise time distribution several very short distributions exist. These distributions occur also very early and could be associated to matrix-fibre debonding and fibre breakage based on the classification presented earlier. Overall, it is evident that different failure mechanisms occur in parallel and from a very early stage. The signals recorded during the unloading phase have features which behave in a similar way as those associated to the loading phase, as figure 4 shows.



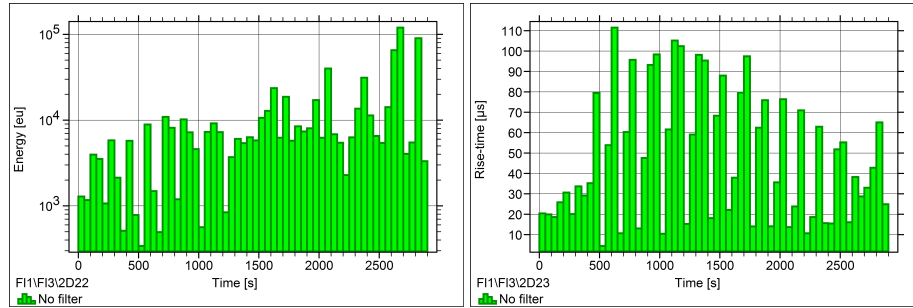


Figure 4. Acoustic emission activity for the unloading phase: Peak Amp (upper left), Duration (upper right), Energy (lower left), Rise-time (lower right)

3.2 Damage development over a fatigue loading range

Figure 5 presents the distribution of number of hits over the loading range for specimen 2. The number of hits recorded during the unloading phase –green distribution- is almost double the number of hits for the loading phase – red distribution- and most of them are found on the lower half of the cycle. On the other hand, for the loading phase, most of the hits are located between 1300 N - 6000 N, followed by the range 6000 N – 8500 N where a notable reduction occurs. Finally, a significant emission rate is observed at the highest loads, between 8500 N – 9000 N.

There are two load ranges, one per phase, where the acoustic emission activity is zero, indicating that there is threshold below and above which, damage is not generated. The thresholds are 1300 N and 8500 N for the loading and unloading phases respectively, see figure 5.

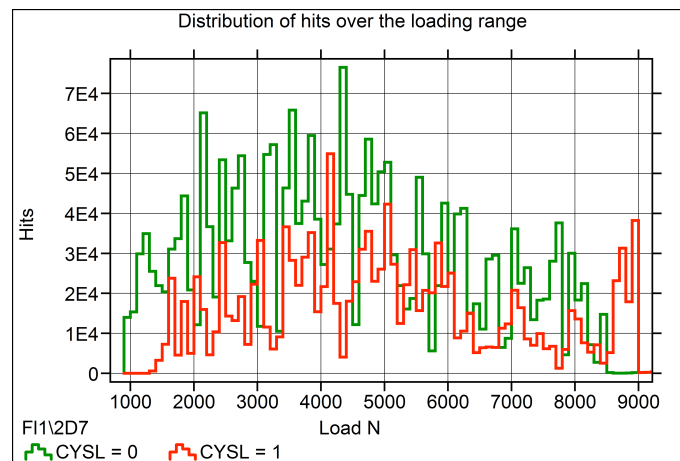


Figure 5. Distribution of number of hits over the load range (green and red indicate the unloading and loading phase respectively) for specimen loaded at 55%

Figure 6 presents the cumulative number of hits over the fatigue life for 4 different loading ranges. Each curve evolves at a different rate, indicating that the maximum and the minimum load where the AE hits are recorded are not constant over the fatigue life. This means that there is a minimum and maximum threshold per cycle, cycle-threshold, and a global threshold for the entire fatigue life, fatigue-thresholds, which in this case is 1300 N and 8500 N.

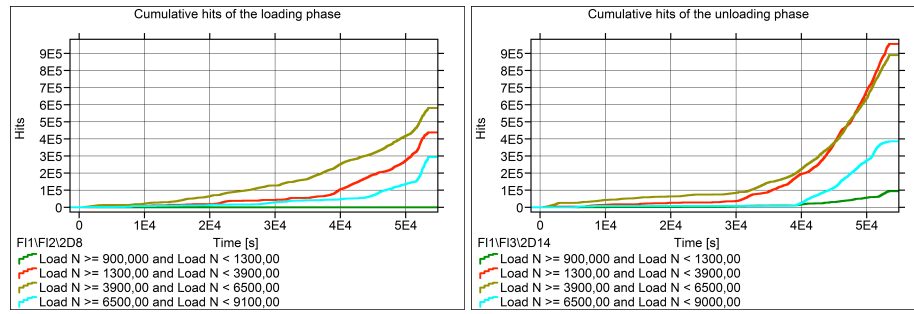


Figure 6. Cumulative number of hits per four loading ranges for the loading (left) and unloading (right) for a specimen loaded at 55%

A similar analysis was performed for the specimens loaded to the higher σ_{\max} . Figure 7 presents the distribution of number of hits over the fatigue loading range. The number of hits are evenly distributed over the loading range for both the loading and unloading phase of the fatigue cycle up to 11000 N, where a significant increase of number of hits is observed. In this case, the number of hits, recorded during the loading phase, is higher than the number recorded during the unloading phase. Similarly, there is a fatigue-threshold at 2000 N, however only for the loading phase. Figure 8 presents the cumulative number of hits for four loading ranges and as their rates evolve differently, similar conclusions to the previous example are drawn.

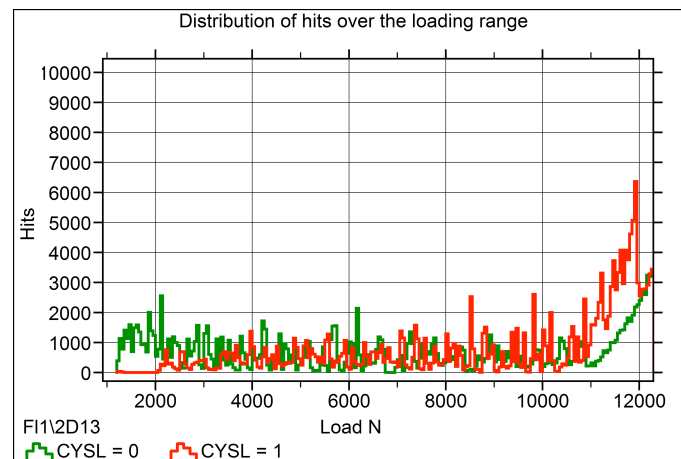


Figure 7. Distribution of number of hits over the load range (green and red indicate the unloading and loading phase respectively) for specimen loaded at 55%

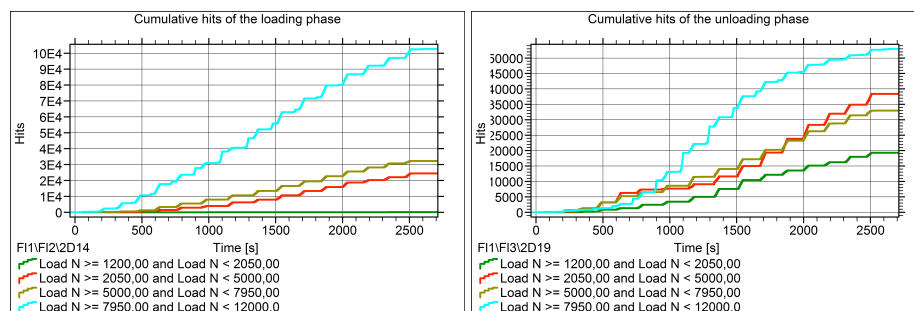


Figure 8. Cumulative number of hits per four loading ranges for the loading (left) and unloading (right) for specimen loaded at 75%

4. Conslusions

A series of T-T fatigue tests of CFRP rectangular specimens with stacking sequeunce $[\pm 45]_{4S}$ was executed, while the AE technique was employed to monitor the fatigue damage accumulation process. The specimens were tested at 55% and 75% of the ultimate strength, with $R=0.1$ and frequency 5 Hz.

The progress of the AE waveforms' features was monitored during the fatigue life of all specimens and it was categorized based on the waveforms' appearance on the loading and unloading phase. For the specimens loaded at the lower σ_{max} , it was observed that the damage accumulation was gradually increased towards the failure, where a significant amount of acoustic emission energy was recorded, except, approximately at 30% and 50% of the fatigue life where a rapid accumulation of damage occurred. On the other hand, for the specimens loaded at the higher lower σ_{max} , the acoustic emission features are levelized from a very early stage, indicating that several failure mechanisms occurred in parallel and developed until the final failure of the specimen.

The acoustic emission activity over the course of a fatigue cycle was examined and it was found that there were thresholds below and above which the acoustic emission was zero, indicating that damage did not generate or propagate during those portions of the cycles. Furthermore, these thresholds are not constant over the fatigue life and change per cycle. These findings support the argument made by the authors that the damage occurs within a portion of the fatigue cycle and this portion may change per cycle.

References

- [1] Reifsnider KL, Talug A. Analysis of fatigue damage in composite laminates. *International Journal of Fatigue*, 2(1):3–11, 1980.
- [2] B. Harris. Fatigue in composites. *Science and Technology of the fatigue Response of Fibre-Reinforced Plastics*. Woodhead Publishing; 2003.
- [3] A. Varvani-Farahani, A. Shirazi. A fatigue damage model for (0/90) FRP composites based on stiffness degradation of 0 and 90 composite plies. *Journal Reinforced Plastic Composites* 2007.
- [4] Y. Zhang, A.P. Vassilopoulos, T. Keller . Stiffness degradation and fatigue life prediction of adhesively-bonded joints for fiber-reinforced polymer composites. *International Journal of Fatigue*. 30(10):1813–20, 2008.
- [5] J.-A. Pascoe, D. Zarouchas, R. Alderliesten, R. Benedictus. Using acoustic emission to understand fatigue crack growth within a single load cycle. *Engineering Fracture Mechanics*, 194: 281-300, 2018.
- [6] A. Marec, J.-H. Thomas, R. El Guerjouma. Damage characterization of polymer-based composite materials: Multivariable analysis and wavelet transform for clustering acoustic emission data. *Mechanical Systems and Signal Processing*. 22: 1444-64, 2008.
- [7] W. Roundi, A. El Mahi, A. El Gharad, J.-L. Rebiere. Acoustic emission monitoring of damage progression in Glass/Epoxy composites during static and fatigue tensile tests. *Applied Acoustics*. 132: 124-34, 2018.